

THERMAL IMBALANCE FORCE MODELING FOR GPS SATELLITES USING THE FINITE ELEMENT METHOD (101)

Yvonne Vigue^{*}, Bob E. Schutz[†], and P. A. M. Abusali[§]

Abstract

Geophysical applications of the Global Positioning System (GPS) require the capability to estimate and propagate satellite orbits with high precision. An accurate model of all the forces acting on a satellite is an essential part of achieving high orbit accuracy. Methods of analyzing the perturbation due to thermal radiation and determining its effects on the long term orbital behavior of GPS satellites are presented. The thermal imbalance force, a non-gravitational orbit perturbation previously considered negligible, is the focus of this paper. The Earth's shadowing of a satellite in orbit causes periodic changes in the satellite's thermal environment. Simulations show that neglecting thermal imbalance in the satellite force model gives orbit errors larger than 10 meters over several days for eclipsing satellites. This orbit mis-modeling can limit accuracy in orbit determination and in estimation of baselines used for geophysical applications.

Nomenclature

A	= surface area
c	= speed of light
C_p	= specific heat
E_r	= energy emitted by a real body, summed over all wavelengths
\vec{f}	= thermal imbalance force per unit area
h	= incident solar radiation received by solar panel
K	= thermal conductivity
m	= satellite mass (in kg)
\hat{n}	= unit vector normal to surface of solar panel

^{*} Member of Technical Staff, Jet Propulsion Laboratory, California Institute of Technology, Pasadena, California 91109, AIAA Member

[†] Professor, Associate Director, Center for Space Research, University of Texas, Austin, Texas 78712

[§] Research Associate, Center for Space Research, University of Texas, Austin, Texas 78712

q	= radiative energy
\vec{r}	= geocentric satellite position vector
r	= radial distance from earth center of mass to satellite
t	= time
T	= temperature
α	= surface absorptivity
ϵ	= emissivity
ρ	= density
ψ	= solar constant
σ	= Stefan-Boltzmann constant
μ	= Earth's gravitational parameter

subscripts

a	= solar panel sun-tracking front side
b	= solar panel back side, no direct sunlight
in	= incoming to the spacecraft
out	= leaving the body
r	= radiative
thermal	= thermal imbalance

1 Introduction

Mismodeling of satellite force parameters can have a significant effect on satellite orbits, especially in orbit prediction. ¹Some applications require the capability to estimate and propagate satellite orbits with high precision. TOPEX precision orbit determination is one example where precise modeling of non-gravitational forces is essential in order to fulfill mission requirements.² Also, some of the observed drag and orbit decay on the spacecraft LAGEOS has been attributed to unmodeled thermal forces.^{3,4} The focus of this analysis was to assess the effects of neglecting thermal re-radiation and mismodeling of non-gravitational forces on satellite orbits. To achieve a

high level of orbit accuracy, an accurate model of all the forces acting on an earth-orbiting satellite is necessary.

Radiative heat transfer between a satellite and its environment is the basis for the thermal force model. A satellite in Earth orbit is continuously illuminated by radiation, most of which comes from the sun. The thermal imbalance force is directly related to the temperature distribution of the satellite in its changing environment. An uneven temperature distribution causes surfaces to re-radiate energy at different rates. Some studies have shown that most of the thermal gradient forces on a TOPEX satellite originate within the spacecraft body.² Whereas, other analyses have shown that the dominant source for thermal re-radiation forces on a G1'S-like satellite is the solar panels due to their large exposed area and low heat capacity.⁵

The satellite's heated body re-radiates energy at a rate that is proportional to its temperature, losing the energy in the form of photons. By conservation of momentum, a net momentum flux out of the body creates a reaction force against the radiating surface, and the net thermal force can be observed as a small perturbation that affects long term orbital behavior of the spacecraft. The partial differential equations and boundary conditions describing the temperature distribution and the heat transfer between surfaces, along with the application of the finite element method are presented in this paper. A brief description of the statistical estimation technique used for studying the effect of the thermal imbalance force on satellite orbits is included.

Radiation and Heat Conduction Formulation

Two types of heat transfer that affect a spacecraft in orbit are radiation and heat conduction. The exchange of energy between the spacecraft and its surroundings is described by radiation heat transfer. Conduction is the transfer of heat by molecular motion within a solid medium. Figure 1 shows the type of heat transfer that affects an orbiting spacecraft.

The rate of radiant energy transfer is given by Stefan-Boltzmann Law:⁶

$$q_r = \epsilon \sigma T^4 \quad (1)$$

By conservation of momentum, the thermal force, or rate of change of momentum for a radiating surface element, assuming a Lambertian surface, is expressed as:⁵

$$d\vec{f}_{\text{thermal}} = -\frac{2}{3} \frac{\epsilon \sigma T_a^4}{c} d\Lambda \hat{n}_a \quad (2)$$

The unit vector in Eq. 2 is defined as normal to and directed out the sun-tracking surface of the solar panel. The differential force must be integrated over the entire surface to determine the complete thermal force:

$$\vec{f}_{\text{thermal}} = -\frac{2\sigma}{3c} \int_{\Omega} \epsilon T_a^4 d\Lambda \hat{n}_a \quad (3)$$

Clearly, thermal forces cannot be computed unless spacecraft surface temperatures are known.

In general, the temperature at any point within a body satisfies the heat equation:⁵

$$K \nabla^2 T = \rho C_p \frac{\partial T}{\partial t} \quad (4)$$

The solution to this second order partial differential equation requires that boundary conditions be specified. The boundary conditions are defined by thermal radiation and heat conduction. As given by the conservation of energy principle, the total amount of energy coming into a surface is equal to the total amount of energy leaving the surface, assuming there is no internally generated or stored energy (no sinks and no sources). The boundary condition for the satellite surface can be obtained by using this condition as:

$$q_{\text{in}} = q_{\text{out}} \quad (5)$$

where q_{in} is the amount of incoming radiative energy due to external sources and internal conduction and q_{out} is the amount of radiative energy leaving the boundary due to re-radiation and conduction. Figure 2 shows the conservation of energy principle, for a satellite solar panel surface.

Using this concept, the boundary conditions for each surface were constructed. The incident radiative solar energy received per unit area per unit time by side a and side b of the solar panel are represented by h_a and h_b :⁵

$$K\Lambda \frac{\partial T_b}{\partial X} = \epsilon_b \sigma \Lambda T_b^4 - h_b \Lambda \quad (6a)$$

$$-K\Lambda \frac{\partial T_a}{\partial X} = \epsilon_a \sigma \Lambda T_a^4 - h_a \Lambda \quad (6b)$$

The actual amount of incident radiative energy received by each side of the solar panel is a function of panel orientation and the orbit of the satellite. The subscript a represents the left boundary in

local coordinates (cold side) and b is the right boundary, which is assumed to be continuously facing the sun during orbit for a GPS-type satellite. The term on the left side of the equal sign in Eqs. (6a) and (6b) is the heat flux, energy per unit time per unit area, in the local x-direction, which is perpendicular to the solar panel face. The values used for some of the parameters described above are shown in Table 1, and are consistent with values used for GPS satellites.

PDE-Protran, a finite element method program, was used to solve the transient heat conduction and radiation problem presented here. PDE-Protran was developed by Granville Sewell and is a general purpose two-dimensional partial differential equation solver.⁷ This software was combined with a program which incorporated material properties, the satellite's orbit orientation, and thermal environment to determine solar panel surface temperatures. Grid points were chosen to divide the solar panel into small sections or "elements" where the temperature of the solar panel was computed for each grid point in one dimension, across the thickness of the solar panel. These grid points coincide with the boundaries between each layer of the solar panel's "sandwiched" materials (shown in Table 2). Accurate and current knowledge of physical parameters such as surface emissivity, thermal conductivity, heat capacity and material density is required. For this analysis, these material properties are assumed to remain constant throughout the satellite's orbit and only the solar radiation environment varies with time as the satellite experiences eclipsing, or shadowing from the sun by the earth. The material parameters directly influence the thermal forces which are calculated and have an effect on the prediction and propagation of the spacecraft trajectory. Also, these material properties may change in time or degrade due to the harsh environment of space.

Orbit Analysis Technique

In this investigation, the equations of motion for an Earth satellite are assumed to include the two body gravitational effect and the thermal imbalance forces only, and are given in vector form by:

$$\ddot{\vec{r}} = -\frac{\mu\vec{r}}{r^3} + \vec{f}_{\text{therm}} \quad (7)$$

and thermal imbalance force perturbing the satellite, \vec{f}_{therm} , is computed as:

$$\vec{F}_{\text{therm}} = \frac{2\sigma A}{3c} (\epsilon_b T_b^4 - \epsilon_a T_a^4) \hat{n}_a \quad (8)$$

The effect of the thermal imbalance force on a satellite can be observed by comparing the perturbed orbit with the unperturbed two body orbit in time. Since there is no closed form analytical solution for the perturbed equations of motion, a numerical integration technique was necessary to solve the ordinary differential equations of motion. The perturbed and unperturbed orbits originate with the same initial conditions and then the displacement between them at a given time can be observed. A least square.s estimation technique is used to determine the state of the satellite in its orbit at a specified epoch.⁹ The initial conditions of one orbit can be adjusted at a given time to eliminate the secular divergence between the perturbed and unperturbed orbits to observe the periodic behavior.

In this analysis, two types of GPS satellite orbits were studied. The satellites of the Global Positioning System are distributed in six evenly spaced orbit planes. When completed, the final constellation will consist of 24 satellites at an orbit altitude of approximately 20,000 km with an orbit period of about 12 hours. In this constellation, most satellites are exposed to full sun light. As the orbit geometry changes, however, some GPS satellites will experience eclipsing or shadowing from the sun by the earth. Both eclipsing and non-eclipsing satellites are the focus of this study. Throughout its orbit, the GPS solar panel maintains a fixed orientation toward the sun. Nodal motion was not considered, since it is not significant for the short time interval of one week used in this study. No internally generated energy was modeled in this study, but the absorbed solar radiation that is converted to electricity was modeled, using the efficiency of the solar panel at 14.1%. Although studies have shown that for a TOPEX satellite, the thermal radiation forces originating with the spacecraft body are twice that due to the spacecraft solar panels, the major source for thermal re-radiation forces on a GPS-like satellite are the spacecraft's thin, large solar panels.^{2,5} Consequently, in this analysis, the GPS satellite's main body was not considered. Other studies are currently considering this problem of modeling thermal re-radiation forces for a complete GPS spacecraft.

Discussion of Results

in order to determine the direction and magnitude. of the thermal force, the surface temperatures were calculated using the finite element method program, Pill{-Protran.⁷ Several simulations were tested. The data input that was required for the simulation is shown in Table 2. This table lists the material properties for a Block II GPS satellite solar panel (Refs. 8, 10-13, 15). The initial conditions included a solar panel orientation perpendicular to the sun, and an initial temperature of 300°K. The time step used in the analysis was 100 seconds (one GPS orbit is approximately 43,200 seconds and the eclipsing period lasts approximately 3200 seconds).

GPS satellites experience an eclipsing season for only a few weeks every year. Eclipsing has a strong effect on the solar radiation environment those satellite.s. This is evident in the temperature Of a GPS satellite solar pane.1 over one orbit shown in Fig. 3. The steady state temperature for the sun-facing side is approximately 317°K and the shaded side is 313°K. These values compare well with the approximate, value of 313°K which has been measured on the cold shaded side of the solar panel for a GPS satellite.^{10,11} The face exposed to the sun has not been directly measured and therefore the temperature difference between surfaces is not well known, but is believed to be approximately 5°K (Refs. 1(1-12, and 14). During the eclipse period, which lasts approximately one hour, there is a decline to a panel temperature of approximately 253°K. Once exiting the shadow region, the solar panels slowly return to their steady state temperatures after approximately 3 hours.

Modeling the coverglass surface accurately has been difficult during this study since that information was not readily available. The thermal conductivity of this fused silica layer is very low as compared to that of two other dominant layers, the aluminum core and solar cell layers,¹² This layer, on the sun-facing side of the solar panel, contributes most of the temperature imbalance primarily because of its low thermal conductivity and high thickness as compared to other solar panel layers, especially the aluminum core. Although it is believed that the solar panel] coverglass layer is transparent to all incident radiation, the material properties from this specific layer of the solar pane.] were not removed from this analysis. It was important to simulate the solar panel as it

exists in orbit to observe the long term orbital effects of the thermal imbalance force on a GPS satellite. This is adequate as long as the correct material properties are used in the analysis.

As an example, two simulations were performed using identical solar panel parameters (values given in Table 2) except for different thermal conductivities for the sun-facing coverglass layer. These simulations are presented to show the sensitivity of the temperature and thermal force calculations to the thermal conductivity of the coverglass. The value for the thermal conductivity given in Test Case 2 shown in Table 3 was used to demonstrate how unrealistic thermal forces can be computed when using incorrect values for the solar panel material properties. Previously, however, this was believed to be the correct value for the thermal conductivity of the fused silica coverglass layer of a GPS satellite solar panel.^{8,13} The results shown in Table 3 describe the steady-state temperatures and thermal accelerations that were computed using the specified values for the coverglass thermal conductivity. Again, both test cases shown in Table 3 are identical except for the value of thermal conductivity for the solar panel coverglass layer.

In this paper, the reference frame is defined as spacecraft-centered radial and along-track components. The along-track component is also referred to as the transverse, or down-track direction, defined in the direction of the satellite velocity vector. Figure 4 shows radial and along-track components of the acceleration due to thermal r-c-radiation over one orbit for an eclipsing satellite. These compare well with studies which have shown unmodeled non-gravitational forces to cause errors of this magnitude.¹⁴ Also, these results were computed using the information presented in Table 2 and described as Test Case 1 in Table 3.

Figure 5 shows the differences between two orbits, one computed using two-body effects only and another trajectory was computed with two-body and thermal imbalance force for a satellite in an eclipsing orbit during one week. The radial rms is 0.5 meters and the along-track rms is 5.2 meters. These results were computed using a technique similar to the method used to predict satellite orbits based on a set of initial conditions and a complete force model of the spacecraft, which could include the solar radiation pressure, and thermal imbalance force. In this case for an eclipsing satellite after seven days, the along-track components differ by approximately 13 meters.

Figure 6 also shows the differences between two orbits, one with two-body effects only and another computed using two-body and thermal imbalance force for a satellite which is not in an eclipsing plane. The radial rms is 0.5 meters and the along-track rms is 1.6 meters. It can be seen from these results that an eclipsing satellite experiences a larger perturbation in the along-track direction over the span of one week, than a satellite which is not in an eclipsing orbit plane. For the non-eclipsing satellite case, after seven days, the along-track difference is approximately 5 meters.

The next two figures represent the results computed using a least squares estimation algorithm in which the simulated observation data contained only the two-body gravitational and thermal imbalance re-radiation forces. The force model used in the estimation algorithm contained the two-body gravitational force model with a solar radiation pressure model to observe the ability of the force model to account for thermal imbalance forces which have been difficult to model but exist in the observations. The best estimate of the satellite epoch state, in the least squares sense, is calculated which includes the satellite position, velocity and a solar radiation pressure scale factor.

Figure 7 shows the orbit fit residuals for a satellite in an orbit plane that is regularly eclipsing. The radial rms is 5 centimeters and the along-track rms is 80 centimeters. After seven days, the along-track orbit error is almost 2 meters. These results show that the solar radiation pressure scale factor in the estimation scheme is capable of absorbing most of the orbit error due to thermal re-radiation, but not all of the orbit error, especially in the along-track direction.

Figure 8 also shows orbit fit residuals for a GPS satellite, the same estimation technique, but the satellite is in a non-eclipsing orbit plane. The radial rms is 9 mm and the along-track rms is 17 centimeters. After seven days, the along-track orbit error is approximately 40 centimeters. Clearly, the eclipsing of the satellites has an influence on the orbit errors, when a thermal re-radiation force is not included in the estimation force model. Larger orbit errors are calculated when the satellite is in an eclipsing orbit plane.

A one week prediction can be made using the satellite state computed for the best least squares estimate in Figure 7 and compared to the best least square estimate for that predicted week.

Studies have shown that, for eclipsing satellites, the quadratic-like growth in the along-track direction can give errors as large as 50 meters after a one week prediction.¹⁶

Concluding remarks

The current analysis has shown that orbit errors larger than 10 meters occur when mismodeling non-gravitational forces such as the thermal imbalance force presented here. A finite element method technique has been used to calculate satellite solar panel temperatures which are used to determine the magnitude and direction of the thermal imbalance force. Although this force may not be responsible for all of the force mismodeling, conditions may work in combination with the thermal imbalance force to produce such accelerations on the order of 10^{-9} m/s^2 . One possible contribution which is currently being studied is the solar panel misalignment, acting together with the thermal imbalance force which may account for much of the unmodeled perturbations. If sub-meter accurate orbits and centimeter-level accuracy for geophysical applications are desired, a time-dependent model of the thermal imbalance force should be used especially when satellites are eclipsing, where the observed errors are larger than for satellites in non-eclipsing orbits. One study has shown that estimating additional stochastic solar radiation parameters improves GPS orbit accuracy significantly, especially for eclipsing satellites.¹⁷ This technique can be used to absorb the orbit error that is caused by mismodeling thermal imbalance forces.

Although modeling the spacecraft solar panels alone may be considered insufficient, thermal force modeling of the entire spacecraft is a complicated problem. This has been done for spacecraft such as TOPEX where precise orbit determination is critical to mission success.² The study presented here, however, focused only on modeling the solar panels where the material composition is not nearly as complex. Also, the problem of radiation absorbed and conducted through the solar panel and re-radiated out is a simple one-dimensional time-dependent heat transfer problem, with no internal heat generation from scientific instruments or electronics.

Non-gravitational perturbations like the thermal imbalance force have been observed for years on satellites like LAGEOS, and are still not completely understood. Thermal forces are dependent on the environment and specifically on such parameters as the satellite mass, cross-sectional area

and material composition. Unfortunately, these parameters can change or degrade with long-term exposure in space. For this reason, it may be more appropriate to estimate stochastic force parameters to represent the thermal re-radiation forces since the nature and rate of material degradation of the satellite in orbit is unknown.¹⁷ The results obtained using the finite element model used in this study agree with the work of others who have conducted similar studies using the finite difference technique to determine spacecraft thermal gradient forces in an effort to improve the satellite force models.

Acknowledgement

The work described in this paper was carried out by the Jet Propulsion Laboratory, California Institute of Technology, under contract with the National Aeronautics and Space Administration. Consulting on PDE-Protran was provided by Granville Sewell of Center for High Performance Computing at The University of Texas at Austin. The authors would like to thank Lt. Randy White of the United States Air Force Global Positioning System Joint Program Office in Los Angeles, California, for his assistance.

References

- ¹ Vigue, Y., "Thermal Imbalance Effects on a GPS Satellite", University of Texas Center for Space Research Technical Memorandum 90-01, Austin, TX, May 1990.
- ² Antreasian, P. G., and G. W. Rosborough, "Prediction of Radiant Energy Forces on the TOPEX/POSEIDON Spacecraft", Journal of Spacecraft and Rockets, Vol. 29, No. 1, Jan.-Feb. 1992, pp. 81-90.
- ³ Slabinski, V. J. "1 ΔGEOS Acceleration Due to Intermittent Solar Heating During Eclipse Periods", American Astronomical Society, Paper No. 3.9, Gaithersburg, MD, Jul. 1988.
- ⁴ Rubincam, D. P., "1 ΔGEOS Orbit Decay Due to Infrared Radiation from Earth", NASA Technical Memorandum 87804, Jan. 1987.
- ⁵ Cook, R. A., "The Effects of Thermal Imbalance Forces on a Simple Spacecraft", University of Texas Center for Space Research Technical Memorandum 89-02, Austin, TX, May 1989.
- ⁶ Chapman, A. J., Heat Transfer, Macmillan Publishing Company, New York, 1984, p. 14.

- 7 Sewell, G., Analysis of a Finite Element Method: PDE/Protran, Springer-Verlag, New York, 1985.
- 8 Lam, Tung T., private communication, Aerospace Corporation, El Segundo, CA, May 1990.
- 9 Tapley, B. "Statistical Orbit Determination Theory", Recent Advances In Dynamical Astronomy, edited by B. Tapley and V. Szebehely, Aug. 1972.
- 10 Pence, W., private communication, Rockwell International, Seal Beach, CA, Oct. 1990.
- 11 Albeck, J., private communication, Spectrolab Corporation, Sylmar, CA, Aug. 1990.
- 12 Marvin, D., private communication, Aerospace Corporation, El Segundo, CA, Jan. 1991.
- 13 Vigue, Y., "Recent Work on the Effects of Thermal Imbalance Forces on a GPS Satellite", University of Texas Center for Space Research Technical Memorandum 90-02, Austin, TX, May 1990, p. 5.
- 14 Fliegel, H.F., T.E. Gallini, and E. R. Swift, "Global Positioning System Radiation Force Model for Geodetic Applications", Journal of Geophysical Research, Vol. 97, No. B1, pp. 559-568, Jan. 1992.
- 15 Rauschenbach, H. S., Solar Cell Array Design Handbook, Van Nostrand Reinhold Company, New York, pp. 467-468 and 493, 1980.
- 16 Schutz, B. and C.S. Ho, P.A.M. Abusali, B.D. Tapley, "Casa Uno GPS Orbit and Baseline Experiments", Geophysical Research Letters, Vol. 17, No. 5, April 1990, pp. 643-646.
- 17 Vigue, Y., S. M. Lichten, R. J. Muellerschoen, G. Blewitt, and M. B. Heflin, "Improved Treatment of GPS Force Parameters in Precise Orbit Determination Applications", AAS paper no. 93-159, Pasadena, CA, Feb. 1993.

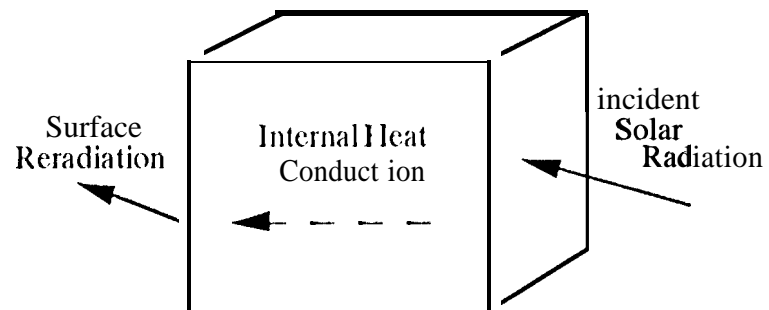


Fig. 1 General Heat Transfer Diagram for a Spacecraft

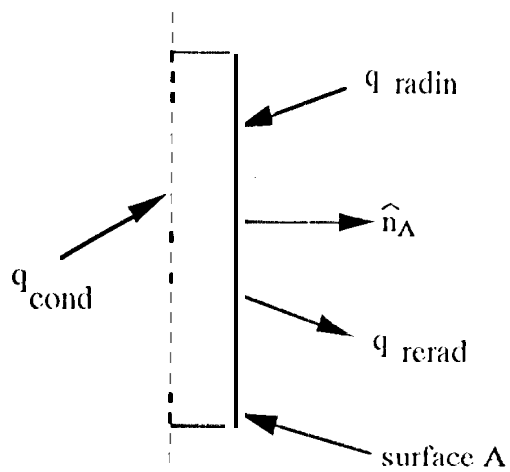


Fig. 2 Conservation of Energy Diagram for a Satellite Surface

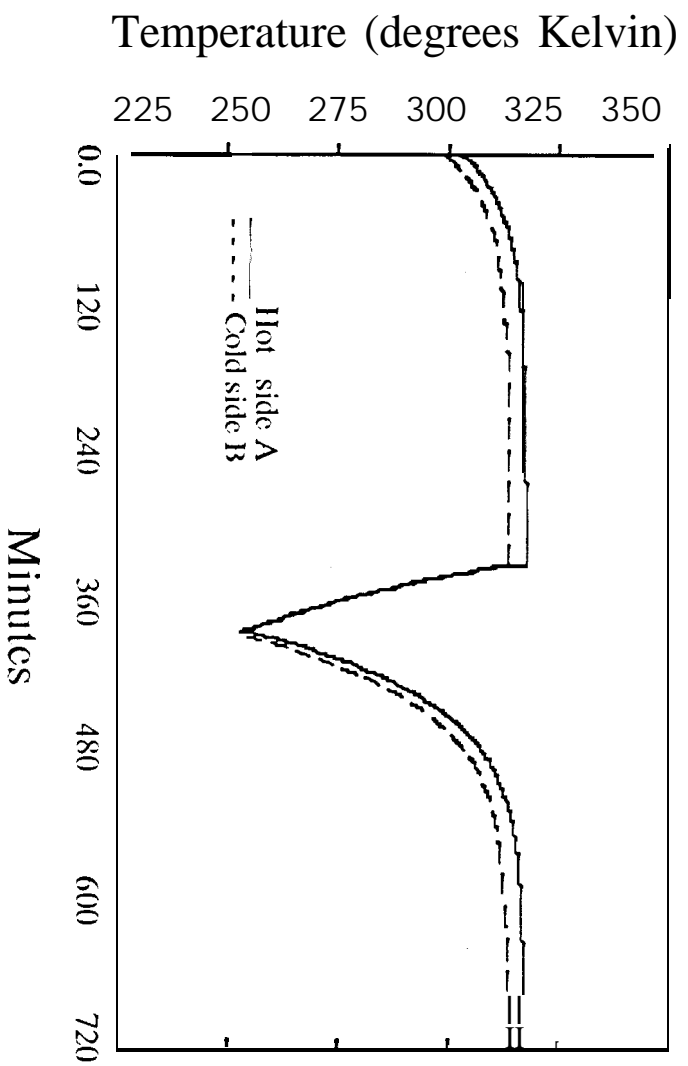


Fig. 3 Temperature history simulation for a GPS solar panel

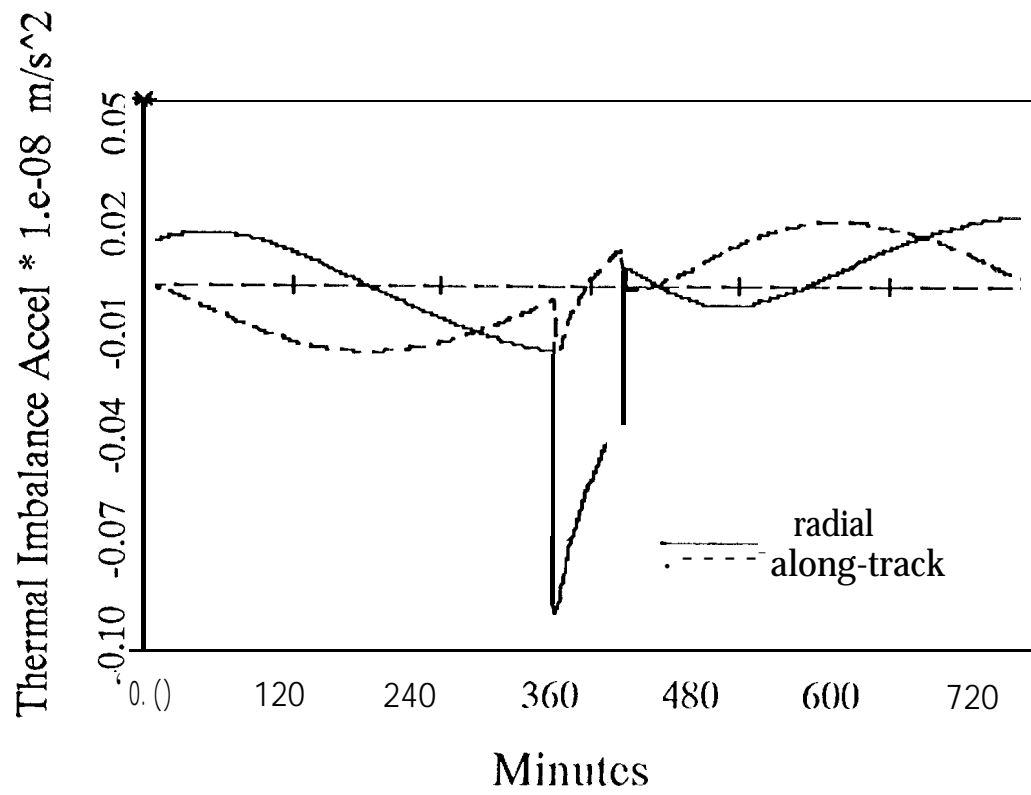


Fig. 4 Radial and along-track components for the thermal force over one orbit

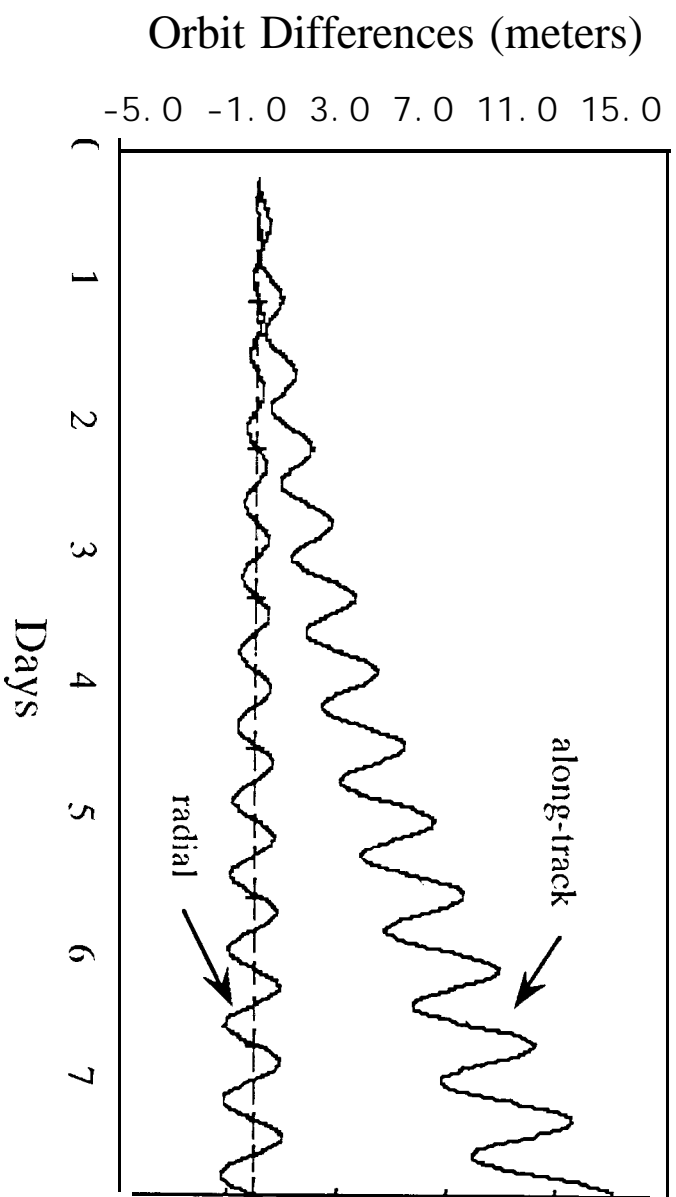


Fig. 5 Radial and along-track orbit differences, eclipsing satellite

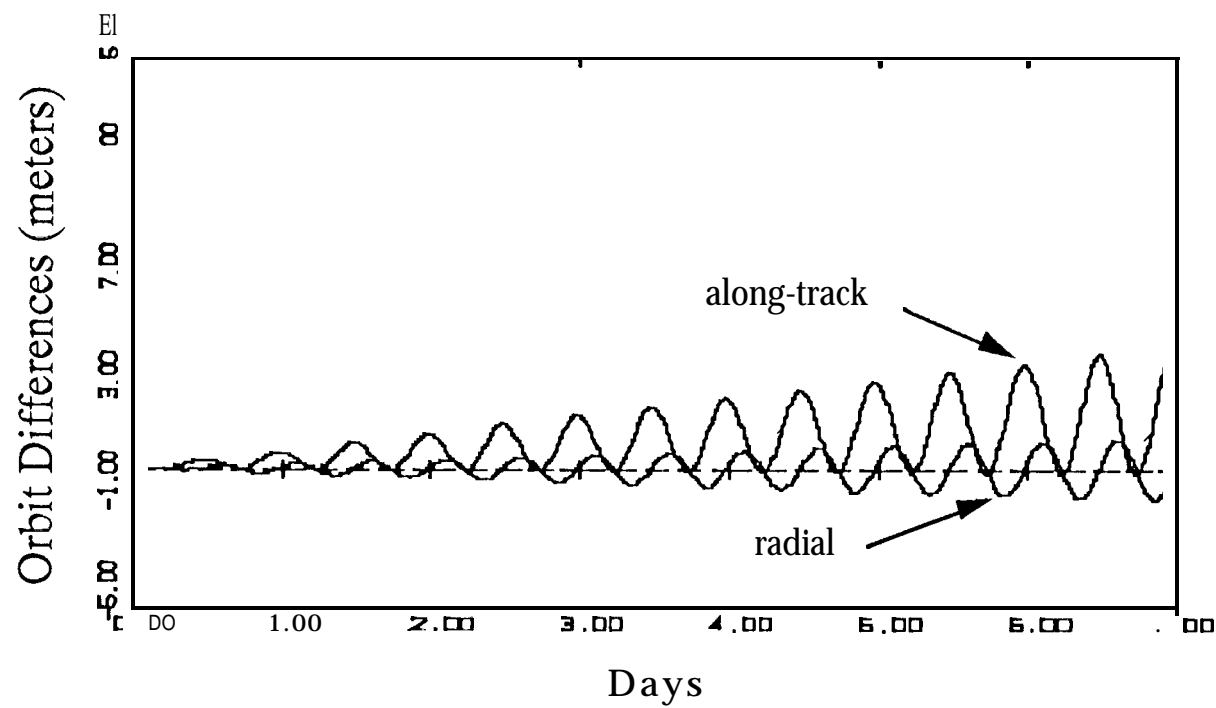


Fig. 6 Radial and along-track orbit differences, non-eclipsing satellite

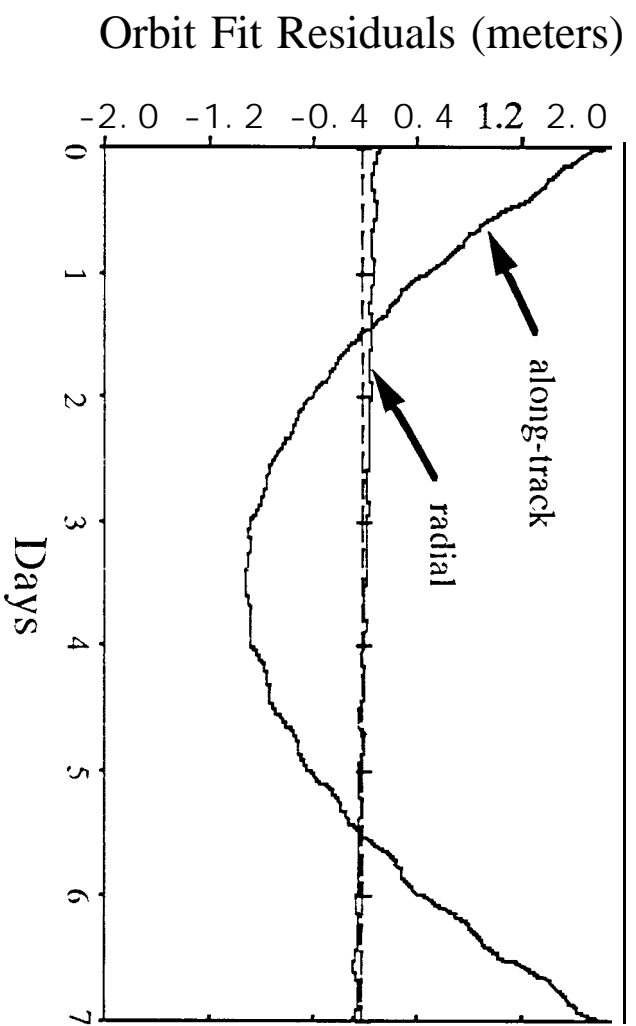


Fig. 7 Orbit fit residuals, with a solar radiation pressure scale factor, eclipsing satellite

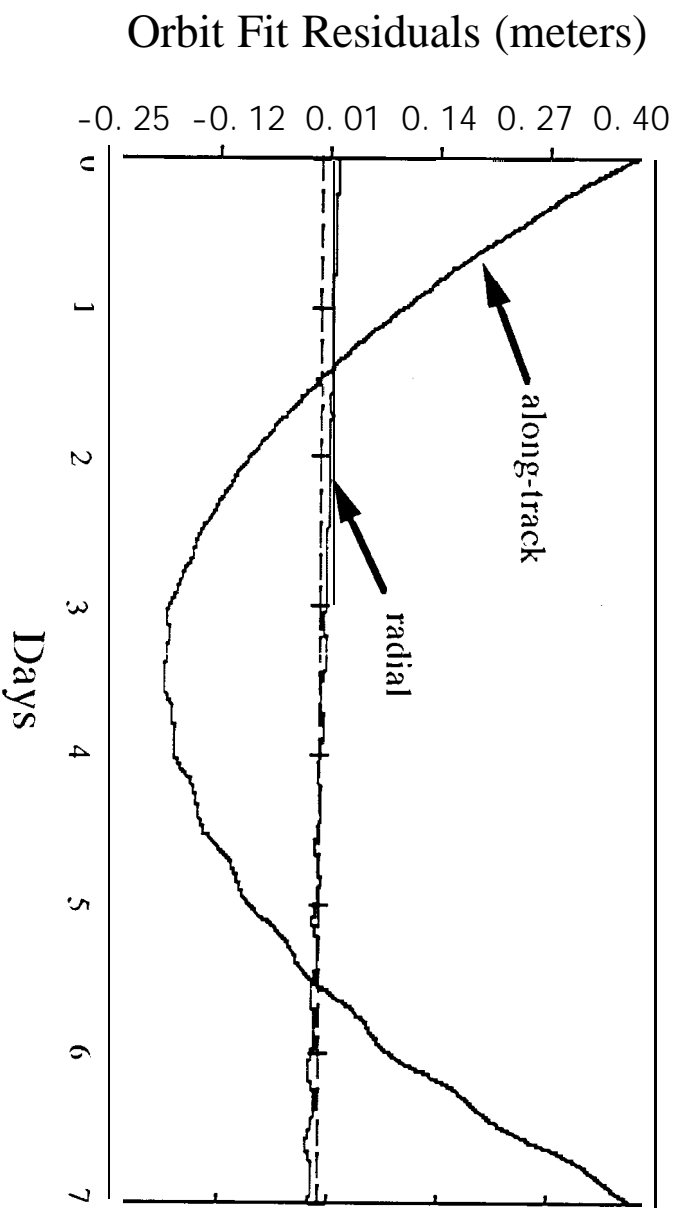


Fig. 8 Orbit fit residuals, a solar radiation pressure scale factor, non-eclipsing satellite

TAIJI.111 GPSTHERMAL AND ORBIT PARAMETERS

Model Parameter	Value
Initial orbit radius:	26,550,000 m
surface emissivity ϵ_a :	0.78
surface emissivity ϵ_b :	0.83
surface absorptivity α_a :	0.77 -14.1 % (panel efficiency)
solar panel surface area -A:	10.8321112
satellite mass - m:	845 kg
initial panel temperature (t = 0) :	300°K
Stefan-Boltzmann constant - σ :	5.6699 E-08 Watts/m ² °K
speed of light -c:	2.998 E+08 m/s
solar constant - ψ :	1368.2 Watts/m ²
total panel thickness (8 layers):	0.01478 m = 0.582 in.

TABLE 2 GPS BLOCK II SOLAR PANEL PROPERTIES

Panel Layer Composition	Thickness meters	Density (kg/m ³)	Specific Heat (J/kg°K)	Thermal Conductivity (W/m *K)
coverglass	0.00749	2186.622	753.624	1.417
adhesive	0.00005	1079.472	1256.04	0.116
solar cell	0.00025	2684.84	711.756	147.994
interconnect cell adh.	0.00018	1051.793	1256.04	0.116
Kapton cocured	0.000076	1162.5(N	1130.436	0.1506
graphite epoxy	0.00019	2186.622	1373.27	0.8706
aluminum core	0.00635	24.91088	1046.7	250.966
graphite epoxy	0.00019	2186.622	1373.27	0.8706

TABLE 3 COVERGLASS THERMAL SIMULATION

Test Case 1	Test Cast 2
$K = 1.417 \text{ W/m}^{\circ}\text{K}$	$K = 0.04327 \text{ W/m}^{\circ}\text{K}$
Hot side $T_a = 317.41 \text{ }^{\circ}\text{K}$	Hot side $T_a = 340.30 \text{ }^{\circ}\text{K}$
Cold side $T_b = 313.66 \text{ }^{\circ}\text{K}$	Cold side $T_b = 285.37 \text{ }^{\circ}\text{K}$
Thermal cc. = 1.88 E-10 m/s²	Thermal Acc. = -8.01 E-9 m/s²

Figure Captions:

Fig. 1 General Heat Transfer Diagram for a Spacecraft

Fig. 2 Conservation of Energy Diagram for a Satellite Surface

Fig. 3 Temperature history simulation for a GPS solar panel

Fig. 4 Radial and along-track components for the thermal force over one orbit

Fig. 5 Radial and along-track orbit differences, eclipsing satellite

Fig. 6 Radial and along-track orbit differences, non-eclipsing satellite

Fig. 7 Orbit fit residuals, with solar radiation pressure scale factor, eclipsing satellite

Fig. 8 Orbit fit residuals, with solar radiation pressure scale factor, non-eclipsing satellite

Table Captions:

Table 1 GPS Thermal and Orbit Parameters

Table 2 GPS Block II Solar Panel Properties

Table 3 Coverglass Thermal Simulation